The required transfer function may be written as follows:

$$\frac{\theta(s)}{\gamma(s)} = \frac{A(s)}{C(s)} \tag{21}$$

The transfer function for the feedback path is given by the following equation:

$$\frac{\theta_f(s)}{\theta(s)} = \frac{1}{\mu}(s + \mu) \tag{22}$$

and hence the open-loop transfer function of the system is simply

$$\frac{\theta_f(s)}{\theta_e(s)} = \frac{\theta(s)}{\theta_e(s)} \frac{\theta_f(s)}{\theta(s)}$$

which becomes on substitution of the results of equations (19) and (22)

$$\frac{\theta_f(s)}{\theta_e(s)} = \frac{a_0 N}{\mu} \frac{A(s)}{C(s)}(s + \mu) \tag{23}$$

By letting

$$G(s) = \frac{a_0}{\mu} \frac{A(s)}{C(s)}(s + \mu) \tag{24}$$

and substituting $s = j\omega$, where $j = \sqrt{-1}$, the open-loop transfer function may be written in a more usable form as follows:

$$\frac{\theta_f(\omega)}{\theta_e(\omega)} = N(\beta_o, \omega)G(\omega) \tag{25}$$

It should be noted that $G(s)$ represents the transfer function of the linear elements in the open-loop system. (See fig. 3.) In a similar manner, N represents the equivalent transfer function for all the nonlinearities in the open loop.

Method for Determining System Stability Graphically

By using equations (19) and (25), the closed-loop transfer function $\theta(s)/\theta_p(s)$ for the system may be formulated as

$$\frac{\theta(s)}{\theta_p(s)} = \frac{\theta(s)/\theta_e(s)}{1 + N\,G(s)} \tag{26}$$

where the numerator is the transfer function of the elements in the forward loop. The characteristic stability equation for the system is obtained by equating the denominator of equation (26) to zero; that is,

$$1 + N\,G(s) = 0 \tag{27}$$

Solutions of this equation represent conditions of marginal (neutral) stability. Rearranging equation (27) and expressing the results in a polar form produces the following equivalent equations which may be solved graphically:

$$\left.\begin{aligned} \left|G(\omega)\right| &= \frac{1}{\left|N(\beta_o,\omega)\right|} \\ \theta_g(\omega) &= 180^\circ - \psi_1(\beta_o,\omega) \end{aligned}\right\} \tag{28}$$

where the substitution $s = j\omega$ has been made.

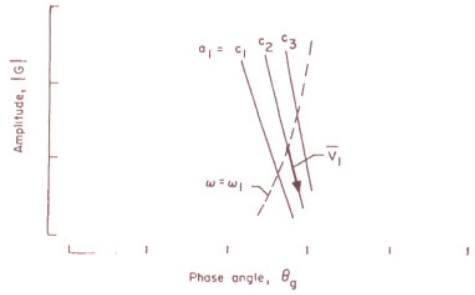

(a) Typical gain-phase plot for $G(\omega)$.

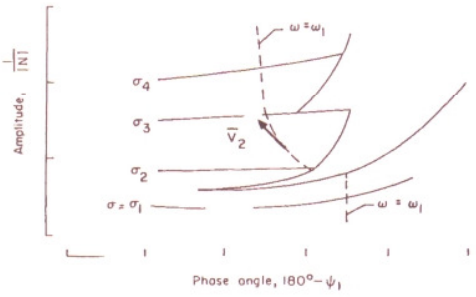

(b) Inverse describing function $1/N$.

Figure 6.- Illustration of graphical solution in gain-phase plane.

In order to effect a graphical solution of equations (28), the amplitude $|G|$ is plotted against the phase angle θ_g with the frequency ω as a parameter. A typical plot is illustrated in part (a) of figure 6 for several values C_1, C_2, and C_3 of the attitude-rate gain a_1. The vector $\bar{V}_1$ is drawn tangent to the $a_1 = C_2$ curve and is directed in the sense of increasing frequency. An inverse describing-function plot is then dimensionalized by selecting a value for the natural frequency ω_n of the control engine and by using equations (10) to convert the constant Ω curves to constant ω curves. A typical inverse describing-function plot is shown in part (b) of figure 6 for several values of the amplitude ratio σ_1, σ_2, ... The vector $\bar{V}_2$ is drawn tangent to the $\omega = \omega_1$ curve and is directed in the sense of increasing amplitude ratio σ (assuming $\sigma_4 > \sigma_3 > \sigma_2 > \sigma_1$) where σ is defined by equations (10).

Once the inverse describing function has been dimensionalized, equations (28) may be solved graphically (ref. 3) by superimposing parts (a) and (b) of figure 6. Solutions are represented by those intersections which occur at a common frequency ω. The procedure is illustrated in part (c) of figure 6. An intersection, that is, a solution, is indicated for a frequency of $\omega = \omega_1$. The amplitude ratio σ

for the solution is between $\sigma = \sigma_2$ and $\sigma = \sigma_3$ and the attitude-rate gain is $a_1 = C_2$.

Solutions of equations (28) determine conditions of marginal stability known as limit cycles. If a limit cycle is stable, the system will return or converge, after a slight disturbance, to the marginal stability condition. If the system diverges, the limit cycle is unstable.

In general, a rigorous definition of stability, that is, whether a solution of equations (28) represents a stable or unstable limit cycle, is difficult to formulate. Instead, an argument is presented based on an intuitive extension of the definition of stability for linear systems. The argument proceeds as follows: Let $\tilde{G}(\omega)$ represent the open-loop transfer function of a linear system. By using the Nyquist stability method, $\tilde{G}(\omega)$ is plotted in the complex plane (for $0 \leqq j\omega < j\infty$) as shown, for example, in part (a) of figure 7. A circle of unit radius is then constructed about the origin and the intersection of this circle with the negative real axis defines the critical point $-1 + j0$. Within the framework of the abbreviated Nyquist method (if it is assumed that the open-loop transfer function $\tilde{G}(\omega)$ is stable), the relative stability of the closed-loop system may be determined by the amount of phase margin ψ present when $G(\omega) = 1$ or rather, when $G(\omega)$ intersects the unit circle. For example, at point A in part (a) of figure 7 the phase margin ψ_A is positive (by definition) and the system is stable, since the Nyquist plot of $G(\omega)$ does not encircle the critical point $-1 + j0$. If $G(\omega)$ intersected the unit circle at point B where the phase margin ψ_B is negative, the closed-loop system would be unstable. In summary the system is stable if the phase margin is positive and unstable if the phase margin is negative. The condition of marginal or neutral stability occurs for zero phase margin.

The preceding ideas may be extended intuitively to a nonlinear system with an

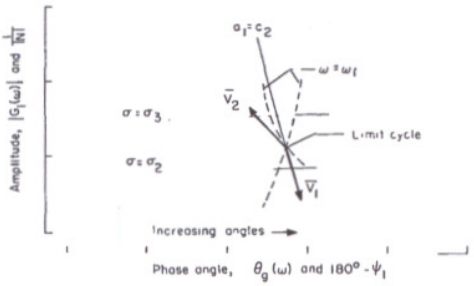

(c) Typical graphical solution resulting when the gain-phase plot and the inverse describing function are superimposed.

Figure 6.- Concluded.

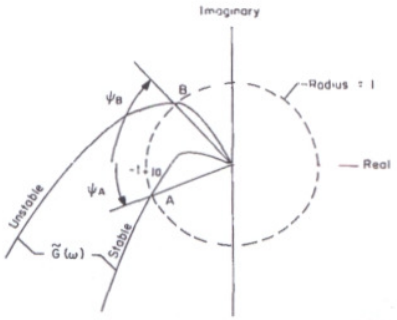

(a) Typical Nyquist plot for a linear system.

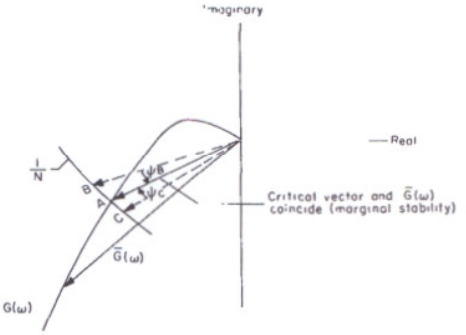

(b) Illustration of the describing function method using a Nyquist plot.

Figure 7.- Comparison of the Nyquist stability method as applied to linear and nonlinear systems.

amplitude- and frequency-dependent describing function. In this case, the critical point is located in the complex plane by the critical vector

$$\frac{1}{\left|N(\beta_o,\omega)\right|}, \angle 180^\circ - \psi_1(\beta_o,\omega)$$

where it is apparent that both the magnitude and direction of this vector vary with β_o and ω. As illustrated in part (b) of figure 7, a solution is shown at point A. Since the solution represents a point of marginal stability (zero phase margin) the critical vector and the $\overline{G}(\omega)$ vector coincide ($\overline{G}$ is the vector which traces out the $G(\omega)$ locus).

Suppose that position A is a solution and that the describing function $N(\beta_o,\omega)$ is such that a minute increase in amplitude (β_o) moves the critical vector to position B. Based on the ideas presented previously for linear systems, one is tempted to interpret the angle ψ_B as a small increment of positive (stable) phase margin and to conclude that the critical vector has shifted its direction so that the closed-loop system is stable for increasing amplitudes. If the system is stable, the solution will eventually return or converge back to position A and, on this basis, the solution may be classified as a stable limit cycle. Conversely, with decreasing amplitudes, the critical vector will shift to position C where the phase margin ψ_C is negative and the system is unstable. As a result, the system will diverge and with increasing amplitudes the solution at position A will again be reached. For a solution to be classified as an unstable limit cycle, it appears that increasing (decreasing) amplitudes must produce negative (positive) phase margins.

Although the preceding argument lacks a rigorous proof, it appears to parallel similar types of reasoning given in the literature (refs. 1, 2, and 3) and is probably applicable to a wide variety of situations. In any case, as an analog computer simulation confirmed, this type of argument did prove to be adequate in classifying the stability boundaries for the system and nonlinearities discussed in this paper.

If reference is made to part (c) of figure 6 and this type of argument is used, the solution (intersection) may be classified as either a stable or unstable limit cycle. By assuming that $\sigma_3 > \sigma_2$, it is apparent that a small increase in the amplitude ratio σ moves the critical vector in the direction of the vector $\overline{V}_2$ and results in a small increment of positive phase margin since θ_g is now slightly greater than the phase angle $180^\circ - \psi_1$. The solution is thus a stable limit cycle.

To conclude this section, the following rule (from ref. 3), which may be helpful in classifying limit cycles, is given. The rule is paraphrased here to fit the specific situation illustrated in part (c) of figure 6. Consider an observer on a curve of constant attitude-rate gain - in this case the $a_1 = C_2$ curve - facing in the direction of increasing frequency, that is, in the direction indicated by vector $\overline{V}_1$. (The vector $\overline{V}_1$, it should be recalled, is

tangent to the $a_1 = C_1$ curve.) Now consider the vector $\overline{V}_2$ which originates on the inverse describing-function plot and is tangent to a line of constant frequency - in this case the $\omega = \omega_1$ curve. (It should be recalled that $\overline{V}_2$ is directed in the sense of increasing amplitude σ.) The rule may be stated as follows: If, to an observer looking along the vector $\overline{V}_1$ the vector $\overline{V}_2$ crosses from left to right, the solution (intersection) represents a stable limit cycle; if it crosses from right to left, the limit cycle is unstable.

DISCUSSION OF RESULTS

In this section the describing-function analysis outlined in the preceding section is employed to determine the stability characteristic of a hypothetical launch vehicle for the maximum dynamic pressure condition of a nominal ascent trajectory. Stability bounds are established for small control engine rotation angles, when the response of the system is essentially linear, by the root-locus method. Then by using the inverse describing function computed previously and representing the linear portion of the open-loop transfer function by gain-phase plots, stability bounds for the nonlinear mode are determined graphically. Finally, an analog computer simulation of the launch-vehicle system is used to verify the describing-function results.

Physical System

The hypothetical launch vehicle analyzed in this study consists of a multi-stage configuration with an overall length to first-stage diameter ratio of about 8.3. The thrust-weight ratio is about 1.25 and the control thrust level was selected as 10 percent of the total booster thrust, that is, $\frac{T_c}{T_b} = 0.1$. The control engine is allowed to rotate through gimbal angles as large as $\pm 90^\circ$, but may be arbitrarily limited at any amplitude up to and including this level. Values for the coefficients required in equations (1) and (2) are given in appendix B.

Linear Stability

For small amplitudes of oscillation the response of the control engine is linear and is governed solely by equation (3). In addition, the coupling of the control thrust with equations (1) and (2) may be satisfactorily approximated by replacing $\sin \beta$ with β (in radians). The transfer function for the control engine is therefore given by the equation

$$\frac{\beta(s)}{\beta_c(s)} = \frac{\omega_n^2}{s^2 + 2\xi\omega_n s + \omega_n^2}$$